ic-2012-02221y

SUPPORTING INFORMATION

The Synthesis and Lewis Acid Properties of $(ReO_3F)_\infty$; the X-ray Crystal Structures of $(HF)_2ReO_3F \cdot HF$ and $[N(CH_3)_4]_2[\{ReO_3(\mu\text{-}F)\}_3(\mu_3\text{-}O)] \cdot CH_3CN$

Maria V. Ivanova, Tobias Köchner, Hélène P. A. Mercier, and Gary J. Schrobilgen*

Department of Chemistry, McMaster University, Hamilton, Ontario L8S 4M1, Canada.

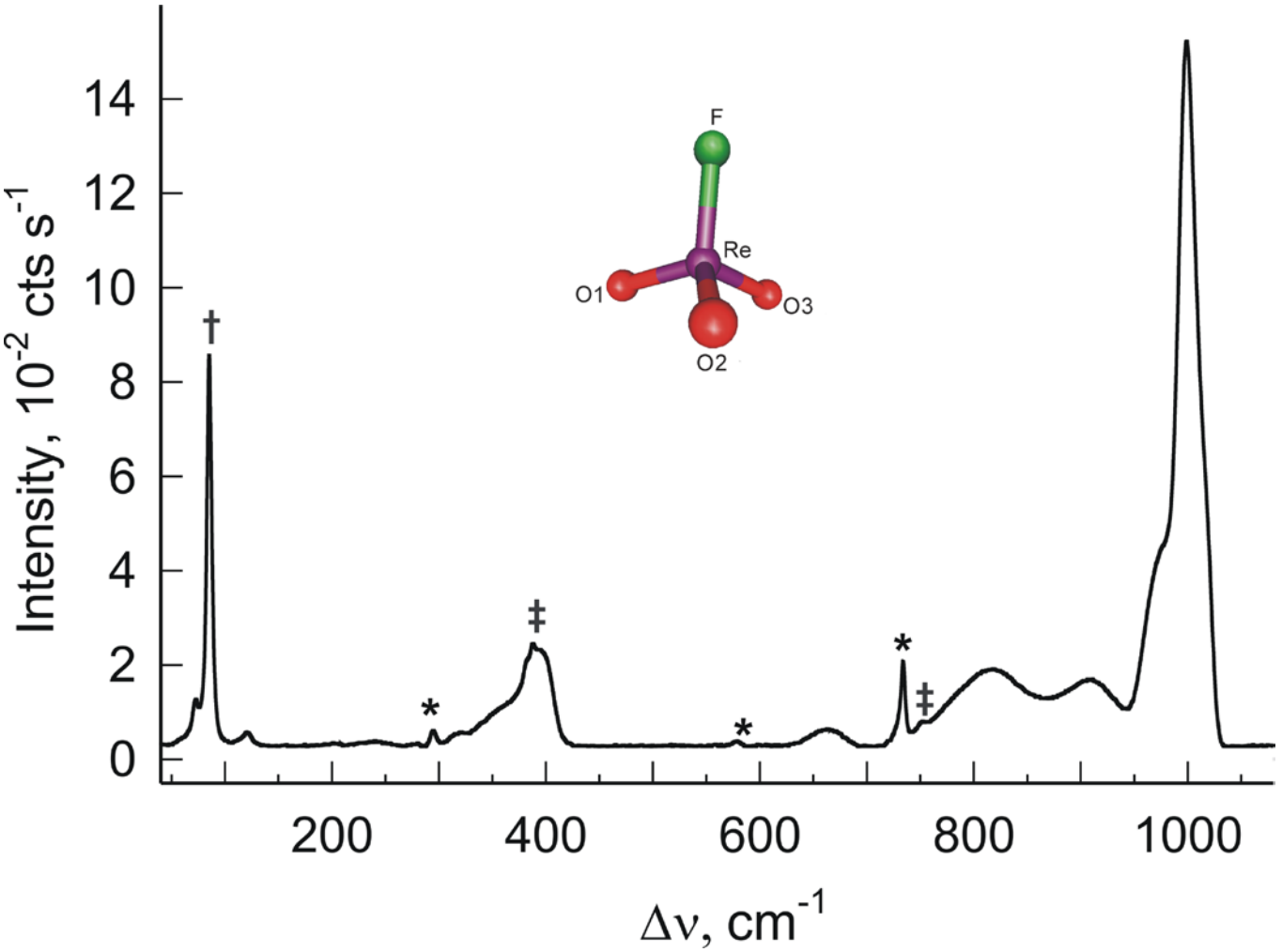

Figure S1. Raman spectrum of $(ReO_3F)_\infty$ recorded at –150 ^oC using 1064-nm excitation. Symbols denote FEP sample tube lines (*), instrumental artifact (†), and overlap of a $(ReO_3F)_\infty$ line with a FEP sample tube line (‡). The geometry of monomeric ReO_3F (C_{3v}) was calculated using the B3LYP/aug-cc-pVTZ(-PP) method.

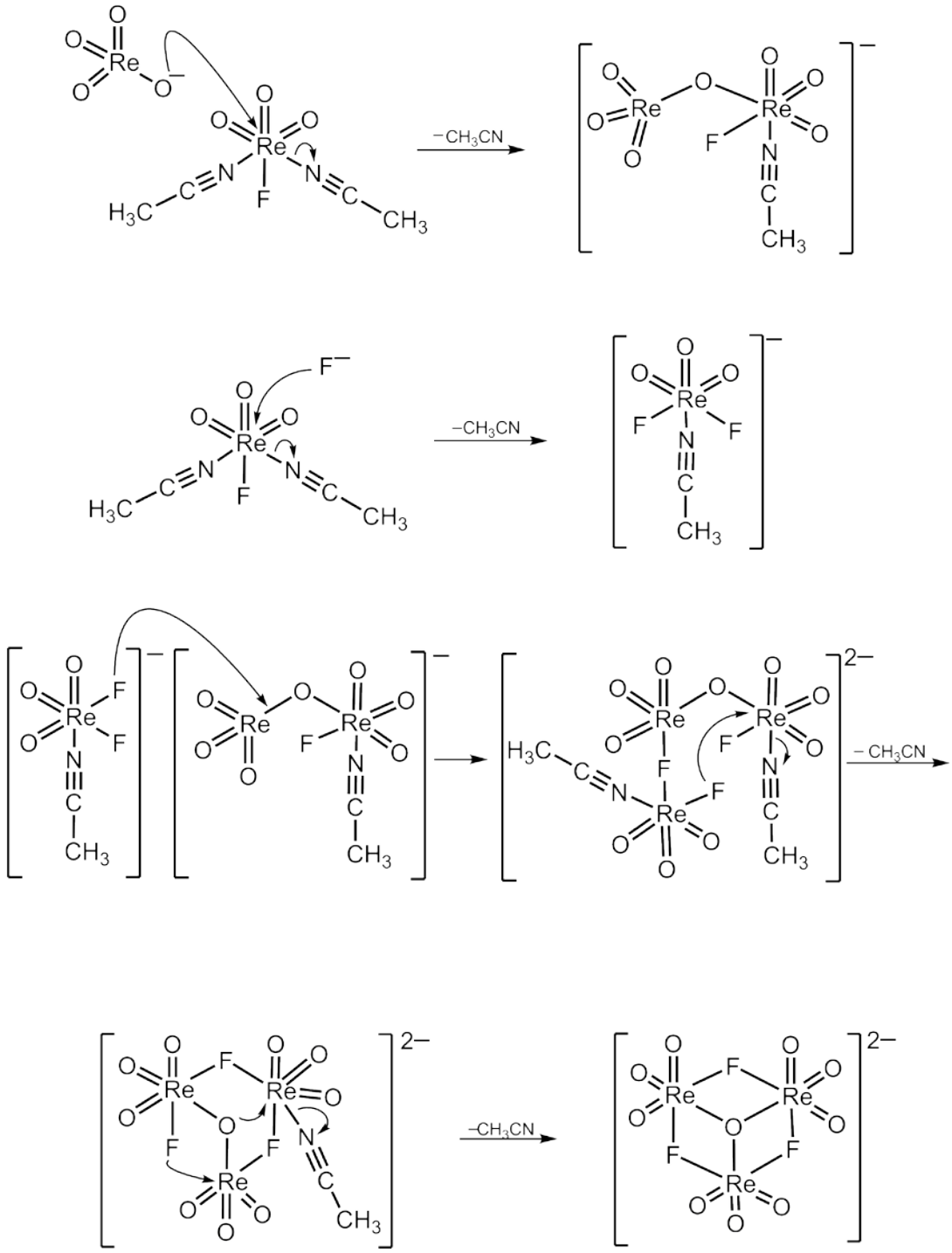

Scheme S1.
An alternative proposed reaction pathway leading to the formation of the $[\{ReO_3(\mu\text{-}F)\}_3(\mu_3\text{-}O)]^{2-}$ anion in CH_3CN solvent. The $[ReO_4]^-$ anion is formed in eq (6).

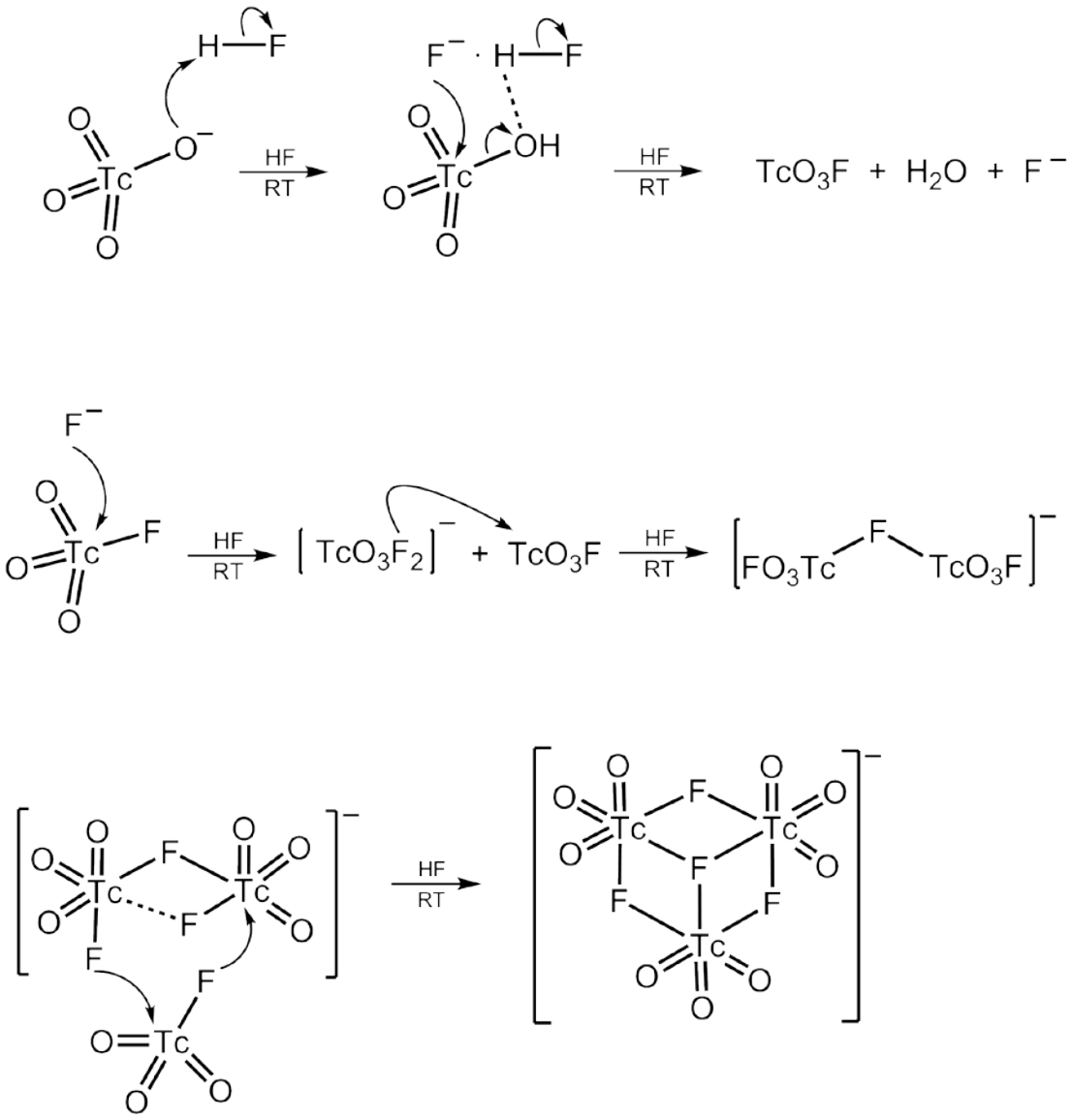

Scheme S2.
A plausible reaction pathway leading to the formation of the $[\{TcO_3(\mu\text{-}F)\}_3(\mu_3\text{-}F)]^-$ anion in aHF solvent. The molecular structure of the $[TcO_3F_2]^-$ anion is presently unknown. Two possible geometries are likely: (1) a trigonal bipyramidal D_{3h} geometry, where the three oxygen atoms lie in the equatorial plane and the fluorine atoms are trans to one another and occupy axial positions that are perpendicular to the TcO_3-plane, and (2) a distorted tetrahedral C_s geometry, where two fluorine atoms, one oxygen atom, and the technetium atom are coplanar and the remaining two oxygen atoms are equidistant from the $TcOF_2$-plane.

Crystal Growth of KF·4HF. Crystals of KF·4HF were grown from a pale yellow solution obtained by dissolving 0.1343 g (0.4641 mmol) of K[ReO_4] in ca. 2 mL of a HF at room temperature. The solution was prepared in a ¼-in. o.d. FEP T-shaped reactor which was pressurized with ca. 1 atm. of dry nitrogen at –78 ^{o}C. The solution was slowly cooled to –71 ^{o}C inside a low-temperature crystal growing apparatus,[41] whereupon colorless plates formed over a period of 4−5 h. A crystal of KF·4HF having dimensions 0.04 x 0.17 x 0.16 mm^3 was selected for a low-temperature X-ray structure determination.

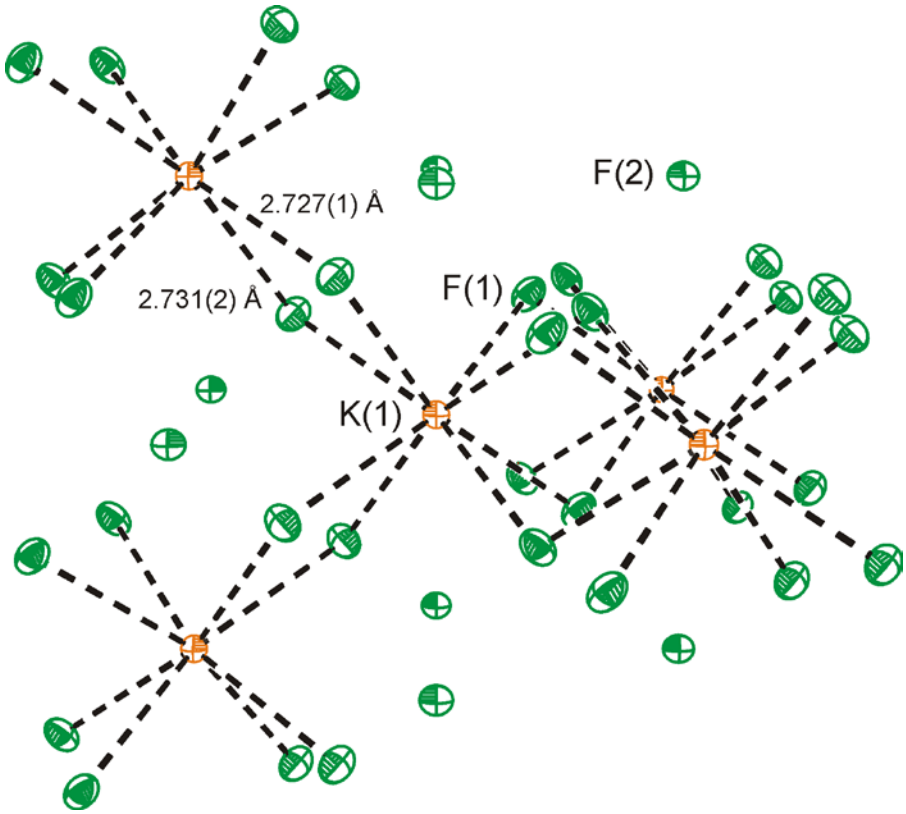

Figure S2. The X-ray crystal structure of KF·4HF. Thermal ellipsoids are shown at the 50% probability level. The "fluorine atoms" that are not coordinated, such as F(2), are HF molecules within the crystal lattice and the "bridging fluorine atoms", such as F(1), are fluoride ions.

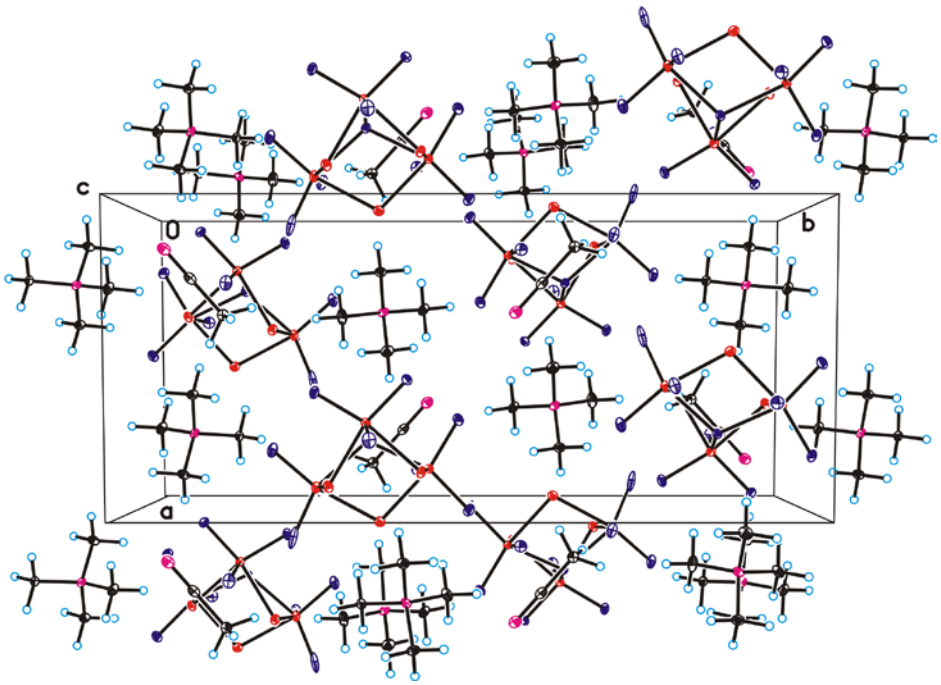

Figure S3. A view of the crystal packing in $[N(CH_3)_4]_2[\{ReO_3(\mu\text{-}F)\}_3(\mu_3\text{-}O)]\cdot CH_3CN$ along the *c*-axis of the unit cell.

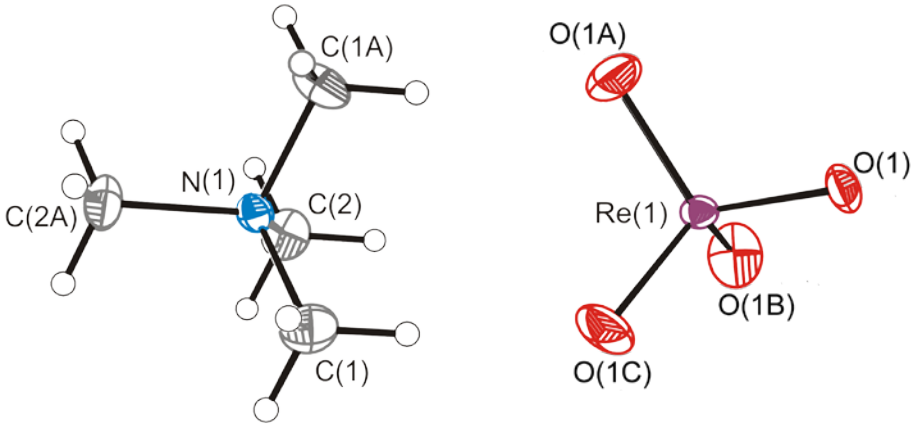

Figure S4. The structural unit in the crystal structure of $[N(CH_3)_4][ReO_4]$. Thermal ellipsoids are shown at the 50% probability level.

Raman Spectrum of $[N(CH_3)_4][ReO_4]$. A low-quality infrared spectrum was previously reported for $[N(CH_3)_4][ReO_4]$[14] that only revealed one intense broad band at ca. 900 cm^{-1} and at least four bands in the 250–350 cm^{-1} region for $[ReO_4]^-$. Reliable Raman data are, however, available for the Na^+,[36] K^+,[35] Rb^+,[36] and $[NH_4]^+$ [35,36] salts of $[ReO_4]^-$. The $[ReO_4]^-$ anion (T_d) is expected to have four Raman-active (A_1, E, $2T_2$), and two infrared-active ($2T_2$) bands. The most intense and highest frequency band of the $[ReO_4]^-$ anion in $[N(CH_3)_4][ReO_4]$ occurs at 964 cm^{-1} and is assigned to ν_s(Re−O) whereas the bands at 899, 909, 928 cm^{-1} are assigned to ν_{as}(Re−O). The bands at 323, 330, 332, and 334 cm^{-1} are assigned to δ(O−Re−O) bending modes. These frequencies are well reproduced by the calculations (Table S1) although the ν_s(Re−O) and ν_{as}(Re−O) stretches are overestimated by about 25 and 15 cm^{-1}, respectively.

Table S1. Experimental Raman Frequencies and Intensities for the $[ReO_4]^-$ Anion in $[N(CH_3)_4][ReO_4]$, $K[ReO_4]$, $[NH_4][ReO_4]$, and $Na[ReO_4]$; and the Calculated Vibrational Frequencies and Intensities for the $[ReO_4]^-$ Anion

exptl[a,b,c,d]					calcd[a,e]	assgnts (T_d)[c]
$[N(CH_3)_4][ReO_4]$[f]	$K[ReO_4]$	$[NH_4][ReO_4]$	$Na[ReO_4]$			$[ReO_4]^-$
964(100)	968(100)	967(100)	957(100)	$\nu_1(A_1)$	989(56)[0]	ν_s(ReO)
928(16) 909(27) 899(14)	927(22) 897(48)	916(14) 894(26)	925(14) 887(39)	$\nu_3(T_2)$	926(13)[276]	ν_{as}(ReO)
334(43) 332 sh	350(35)	356(20)	376 sh 374(17)	$\nu_2(E)$	336(6)[0]	$\delta(O_1ReO_2) + \delta(O_3ReO_4)$
330 sh 323(11)	337(34) 331(11)	343(30) 327 sh	333(18) 320(5)	$\nu_4(T_2)$	333(1)[12]	$\delta(O_1ReO_2) + \delta(O_1ReO_4) - \delta(O_1ReO_3)$

[a]Frequencies are given in cm^{-1}. [b]Values in parentheses denote relative Raman intensities. Raman spectra were recorded in FEP sample tubes at –150 °C using 1064-nm excitation. [c]The abbreviations denote shoulder (sh), stretch (ν), bend (δ), symmetric (s), and asymmetric (as). [d]This work. [e]Values in parentheses denote calculated Raman intensities ($Å^4\ u^{-1}$). Values in square brackets denote calculated infrared intensities (km mol^{-1}). The B3LYP/aug-cc-pVTZ(-PP) method was used. [f]The $[N(CH_3)_4]^+$ cation modes were observed at ν_8(E), 377(1); $\nu_{19}(T_2)$, 463(5), 460(5), 455(5); $\nu_3(A_1)$, 750(3), 757(12); $\nu_{18}(T_2)$, 952(18), 949(8), 943(1); ν_7(E), 1174(1), 1182(2); $\nu_{17}(T_2)$, 1285(1), 1288(2); $\nu_{16}(T_2)$, 1407(5), 14013(3); $\nu_2(A_1)$, ν_6(E), 1461(9), 1467(8); $\nu(CH_3)$ and combination bands, 2801(4), 2810(4), 2904(3), 2915(5), 2953(21), 2962(6), 2992sh, 3026(11), 3034(30) cm^{-1}.

Table S2. Correlation Diagram for the Vibrational Modes of $(HF)_2ReO_3F$ in $(HF)_2ReO_3F \cdot HF$ [a]

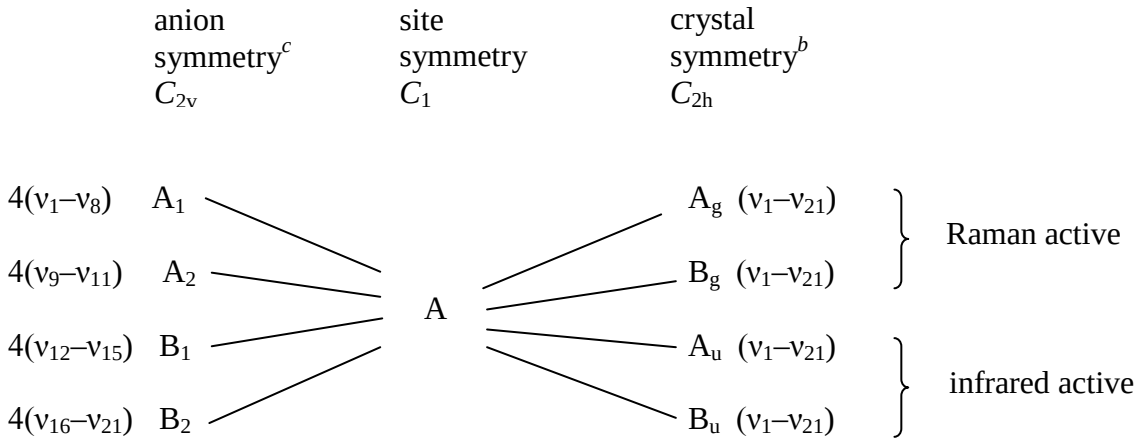

[a]The irreducible representations are $\Gamma = 8A_1 + 4B_1 + 3A_2 + 6B_2$ for $(HF)_2ReO_3F$. [b]The crystallographic space group is $P2_1/c$ with $Z = 4$. [c]The anion (C_{2v}) symmetry is the local symmetry observed in the crystallographic unit cell.

Table S3. Correlation Diagram for the Vibrational Modes of the $[\{ReO_3(\mu\text{-}F)\}_3(\mu_3\text{-}O)]^{2-}$ Anion[a] in $[N(CH_3)_4]_2[\{ReO_3(\mu\text{-}F)\}_3(\mu_3\text{-}O)]\cdot CH_3CN$

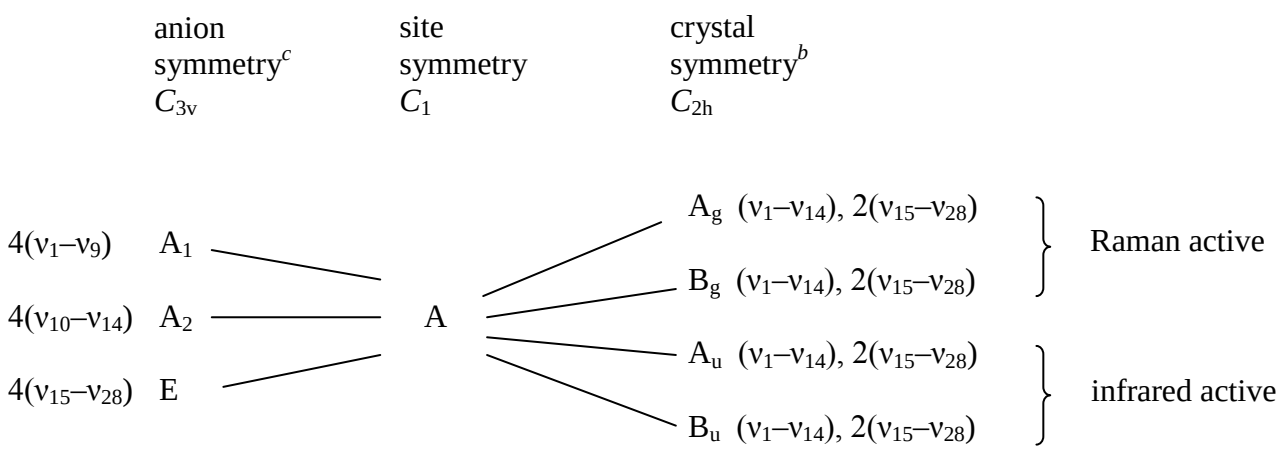

[a]The irreducible representations are $\Gamma = 9A_1 + 5A_2 + 14E$ for the $[\{ReO_3(\mu\text{-}F)\}_3(\mu_3\text{-}O)]^{2-}$ anion. [b]The crystallographic space group is $P2_1/c$ with $Z = 4$. [c]The anion symmetry (C_{3v}) is the symmetry observed in the crystallographic unit cell and for the optimized geometry in the gas phase.

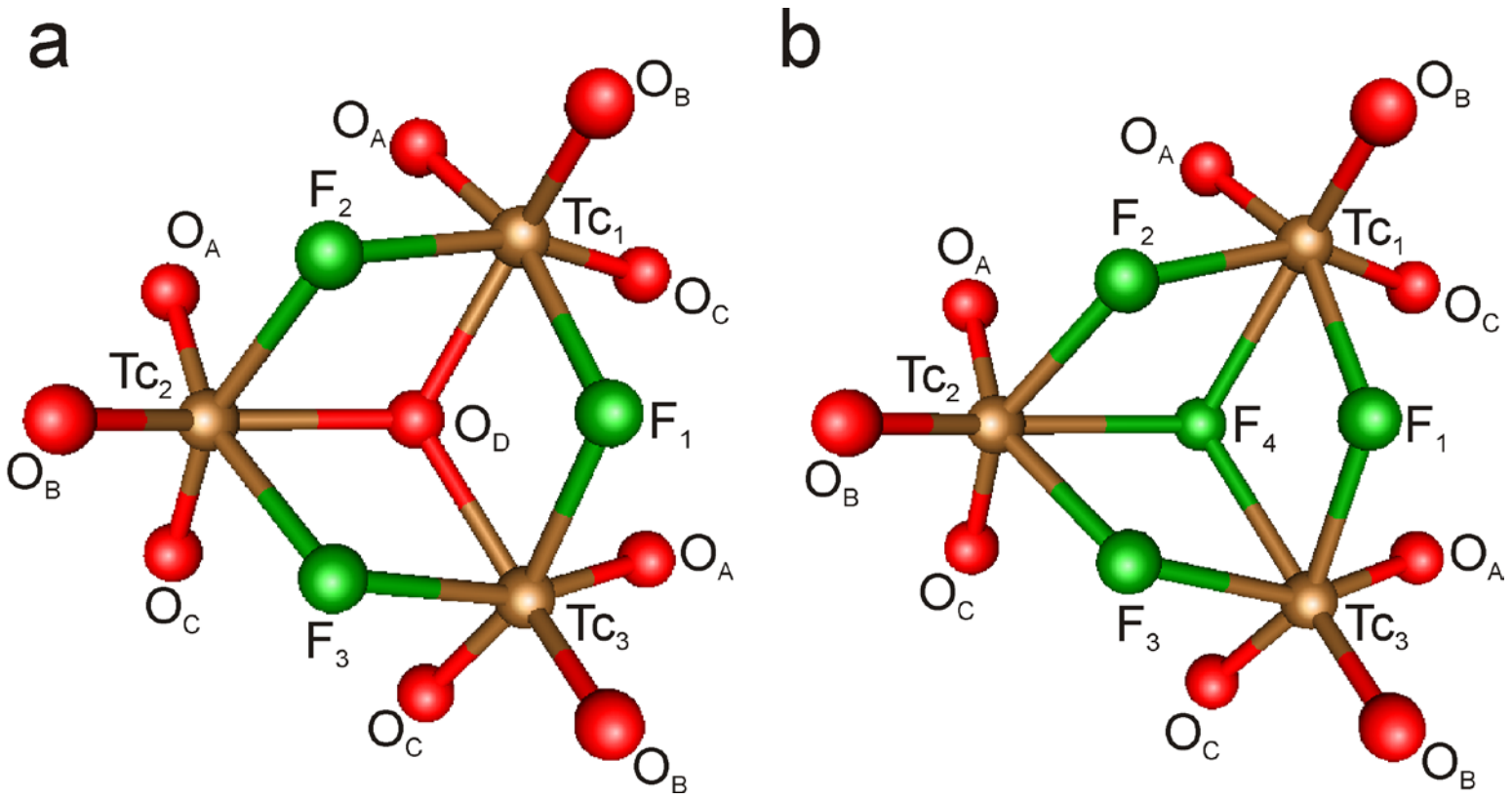

Figure S5. The calculated structures of the (a) $[\{TcO_3(\mu\text{-}F)\}_3(\mu_3\text{-}O)]^{2-}$ and (b) $[\{TcO_3(\mu\text{-}F)\}_3(\mu_3\text{-}F)]^{-}$ anions. The B3LYP/aug-cc-pVTZ(-PP) method was used.

Table S4. Calculated Vibrational Frequencies and Infrared and Raman Intensities for the $[\{TcO_3(\mu\text{-}F)\}_3(\mu_3\text{-}O)]^{2-}$ and $[\{TcO_3(\mu\text{-}F)\}_3(\mu_3\text{-}F)]^{-}$ Anions

$[\{TcO_3(\mu\text{-}F)\}_3(\mu_3\text{-}O)]^{2-}$		assgnts (C_{3v})[c]	$[\{TcO_3(\mu\text{-}F)\}_3(\mu_3\text{-}F)]^{-}$	
calcd[a,b]			calcd[a,b]	
988(173)[94]	$\nu_1(A_1)$	$\nu(Tc_1O_AO_BO_C) + \nu(Tc_2O_AO_BO_C) + \nu(Tc_3O_AO_BO_C)$	$\nu_1(A_1)$	1018(166)[15]
972(5)[197]	$\nu_{10}(E)$	$\nu(Tc_1O_AO_BO_C) - \nu(Tc_2O_AO_BO_C) + \nu(Tc_3O_AO_BO_C)$	$\nu_{10}(E)$	1009(2)[91]
957(27)[521]	$\nu_2(A_1)$	$\nu(Tc_1O_B) + \nu(Tc_2O_B) + \nu(Tc_3O_B)$	$\nu_2(A_1)$	997(6)[482]
960(36)[248]	$\nu_{11}(E)$	$\nu(Tc_1O_A) - \nu(Tc_1O_C) - \nu(Tc_2O_A) + \nu(Tc_2O_C)$	$\nu_{11}(E)$	993(28)[256]
935(54)[112]	$\nu_{12}(E)$	$\nu(Tc_1O_B) - \nu(Tc_2O_B) + \nu(Tc_2O_A) + \nu(Tc_2O_C) - \nu(Tc_1O_A) - \nu(Tc_1O_C)$	$\nu_{12}(E)$	981(25)[66]
551(7)[222]	$\nu_{13}(E)$	$[\nu(Tc_1O_D) + \nu(Tc_3O_D) - \nu(Tc_2O_D)] + [\nu(Tc_1F_1) + \nu(Tc_3F_1) - \nu(Tc_1F_2) - \nu(Tc_2F_2)]$		
499(2)[2]	$\nu_3(A_1)$	$[\nu(Tc_1O_D) + \nu(Tc_2O_D) + \nu(Tc_3O_D)] + [\nu(Tc_1F_1) + \nu(Tc_3F_1) + \nu(Tc_2F_3) + \nu(Tc_3F_3) + \nu(Tc_1F_2) + \nu(Tc_2F_2)]$		
		$[\nu(Tc_2F_4) + \nu(Tc_3F_4)] + [\nu(Tc_1F_1) - \nu(Tc_3F_1) + \nu(Tc_1F_2) - \nu(Tc_2F_2)]$	$\nu_{13}(E)$	471(1)[243]
		$[\nu(Tc_1F_4) + \nu(Tc_2F_4) + \nu(Tc_3F_4)] + [\nu(Tc_1F_1) + \nu(Tc_3F_1) + \nu(Tc_2F_3) + \nu(Tc_3F_3) + \nu(Tc_1F_2) + \nu(Tc_2F_2)] + \delta(O_AO_BTc_1O_C) + \delta(O_AO_BTc_2O_C) + \delta(O_AO_BTc_3O_C)$	$\nu_3(A_1)$	438(3)[17]
		$[\nu(Tc_1F_4) + \nu(Tc_2F_4) + \nu(Tc_3F_4)] + [\nu(Tc_1F_1) + \nu(Tc_3F_1) + \nu(Tc_2F_3) + \nu(Tc_3F_3) + \nu(Tc_1F_2) + \nu(Tc_2F_2)] + [\delta(O_ATc_1O_B) + \delta(O_ATc_2O_B) + \delta(O_ATc_3O_B)]$	$\nu_4(A_1)$	406(4)[3]
420(2)[18]	$\nu_4(A_1)$	$\delta(O_AO_BTc_1O_C) + \delta(O_AO_BTc_2O_C) + \delta(O_AO_BTc_3O_C) + [\nu(Tc_1O_D) + \nu(Tc_2O_D) + \nu(Tc_3O_D)]$		
408(2)[86]	$\nu_{14}(E)$	$[\nu(Tc_1O_D) + \nu(Tc_2O_D) - \nu(Tc_3O_D)] + [\nu(Tc_1F_1) - \nu(Tc_3F_1) + \nu(Tc_2F_3) - \nu(Tc_3F_3)] + [\delta(O_AO_BTc_1O_C) + \delta(O_AO_BTc_2O_C) + \delta(O_AO_BTc_2O_C)]$		
		$[\delta(O_ATc_1O_C) - \delta(O_ATc_2O_C)] + \delta(O_BTc_1F_1F_2) - \delta(O_BTc_2F_3F_2)]$	$\nu_{14}(E)$	400(3)[<1]
		$\delta(O_AO_CRe_1O_B) + \delta(O_AO_CRe_2O_B) + \delta(O_AO_CRe_3O_B) + [\nu(Tc_1F_4) + \nu(Tc_2F_4) + \nu(Tc_3F_4)] + [\nu(Tc_1F_1) + \nu(Tc_3F_1) + \nu(Tc_2F_3) + \nu(Tc_3F_3) + \nu(Tc_1F_2) + \nu(Tc_2F_2)]$	$\nu_5(A_1)$	390(3)[16]
388(6)[8]	$\nu_5(A_1)$	$[\delta(O_ATc_1O_B) - \delta(O_CTc_1O_B) + \delta(O_ATc_2O_B) - \delta(O_CTc_2O_B) + \delta(O_ATc_3O_B) - \delta(O_CTc_3O_B)] + [\nu(Tc_1F_1) - \nu(Tc_3F_1) + \nu(Tc_2F_3) - \nu(Tc_3F_3) - \nu(Tc_1F_2) + \nu(Tc_2F_2)]$		
398(1)[5]	$\nu_{15}(E)$	$[\delta(O_AO_BTc_1O_C) + \delta(O_AO_BTc_2O_C) - \delta(O_ATc_3O_C)] + [\nu(Tc_1F_1) - \nu(Tc_3F_1) + \nu(Tc_2F_3) - \nu(Tc_3F_3)$		
		$[\delta(O_AO_BTc_1O_C) + \delta(O_AO_BTc_2O_C) - \delta(O_ATc_3O_C)] + [\nu(Tc_1F_4) + \nu(Tc_2F_4) - \nu(Tc_3F_4)] + [\nu(Tc_1F_1) + \nu(Tc_3F_1) + \nu(Tc_2F_3) + \nu(Tc_3F_3) - \nu(Tc_1F_2) - \nu(Tc_2F_2)]$	$\nu_{15}(E)$	390(4)[1]
379(4)[47]	$\nu_{16}(E)$	$[\delta(O_ATc_1O_B) - \delta(O_CTc_1O_B) + \delta(O_ATc_2O_C) - \delta(O_ATc_3O_B) - \delta(O_CTc_3O_B)] + [\nu(Tc_3F_1) + \nu(Tc_1F_1)] - [\nu(Tc_1F_2) + \nu(Tc_2F_2)] + [\nu(Tc_2F_3) + \nu(Tc_3F_3)]$		
		$[\delta(O_AO_BTc_1O_C) - \delta(O_AO_BTc_2O_C)]$	$\nu_{16}(E)$	378(<0.1)[<0.1]
376(1)[9]	$\nu_{17}(E)$	$\delta(O_CTc_1O_A) - \delta(O_ATc_2O_B) + \delta(O_BTc_2F_3) + \delta(O_BTc_1F_1F_2)$		
		$[\delta(O_ATc_1O_B) - \delta(O_CTc_1O_B) + \delta(O_ATc_2O_B) - \delta(O_CTc_2O_B)] + [\nu(Tc_1F_4) + \nu(Tc_2F_4) - \nu(Tc_3F_4)] + [\nu(Tc_3F_1) + \nu(Tc_1F_1)] - [\nu(Tc_1F_2) + \nu(Tc_2F_2)] - [\nu(Tc_2F_3) + \nu(Tc_3F_3)]$	$\nu_{17}(E)$	369(2)[12]
365(2)[15]	$\nu_6(A_1)$	$[\rho_w(O_ATc_1O_C) + \rho_w(O_ATc_2O_C) + \rho_w(O_ATc_3O_C)] + [\nu(Tc_1F_2) + \nu(Tc_2F_2)] + [\nu(Tc_2F_3) + \nu(Tc_3F_3)] + [\nu(Tc_3F_1) + \nu(Tc_1F_1)]$		

Table S4. (continued...)

		$\rho_w(O_ATc_1O_C) + \rho_w(O_ATc_2O_C) + \rho_w(O_ATc_3O_C) + [\nu(Tc_1F_2) + \nu(Tc_2F_2)] + [\nu(Tc_2F_3) + \nu(Tc_3F_3)] + [\nu(Tc_3F_1) + \nu(Tc_1F_1)] + [\nu(Tc_1F_4) + \nu(Tc_2F_4) + \nu(Tc_3F_4)]$	$\nu_6(A_1)$	356(<1)[14]
		$[\nu(Tc_1F_2) + \nu(Tc_2F_2)] + [\nu(Tc_2F_3) + \nu(Tc_3F_3)] + [\nu(Tc_3F_1) + \nu(Tc_1F_1)] - [\nu(Tc_1F_4) + \nu(Tc_2F_4) + \nu(Tc_3F_4)] + [\nu(Tc_3F_1) + \nu(Tc_1F_1)] - [\nu(Tc_1F_2) + \nu(Tc_2F_2)] + [\nu(Tc_2F_3) + \nu(Tc_3F_3)]$	$\nu_7(A_1)$	278(1)[9]
252(7)[<1]	$\nu_7(A_1)$	$[\nu(Tc_1F_2) + \nu(Tc_2F_2)] + [\nu(Tc_2F_3) + \nu(Tc_3F_3)] + [\nu(Tc_3F_1) + \nu(Tc_1F_1)]$		
321(3)[14]	$\nu_{18}(E)$	$[\delta(O_ATc_1O_B) - \delta(O_BTc_1O_C) + \delta(O_BTc_2O_C) - \delta(O_BTc_2O_C)] + [\nu(Tc_1F_1) + \nu(Tc_3F_1) + \nu(Tc_2F_3) + \nu(Tc_3F_3)] + [\nu(Tc_1F_4) + \nu(Tc_2F_4) + \nu(Tc_3F_4) - \nu(Tc_1F_2) - \nu(Tc_2F_2)]$		
		$[\rho_w(O_ATc_2O_C) + \rho_w(O_ATc_3O_C)] + [\nu(Tc_1F_1) + \nu(Tc_3F_1) + \nu(Tc_2F_3) + \nu(Tc_3F_3)] + [\nu(Tc_2F_4) + \nu(Tc_3F_4) - \nu(Tc_1F_4)]$	$\nu_{18}(E)$	275(2)[52]
250(1)[6]	$\nu_{19}(E)$	$[\rho_r(O_ATc_1O_C) + \rho_r(O_ATc_3O_C)] + [\nu(Tc_1F_2) + \nu(Tc_2F_2)] + [\nu(Tc_2F_3) + \nu(Tc_3F_3)] - [\nu(Tc_3F_1) + \nu(Tc_1F_1)]$		
		$[\rho_r(O_ATc_1O_B) + \rho_r(O_ATc_2O_B) + \rho_r(O_ATc_3O_C)] + [\nu(Tc_2F_3) + \nu(Tc_3F_3)] - [\nu(Tc_2F_4) + \nu(Tc_3F_4) - \nu(Tc_1F_4)]$	$\nu_{19}(E)$	257(<1)[1]
202(3)[1]	$\nu_8(A_1)$	$[\nu(Tc_1F_2) + \nu(Tc_2F_2)] + [\nu(Tc_2F_3) + \nu(Tc_3F_3)] + [\nu(Tc_3F_1) + \nu(Tc_1F_1)] + [\nu(Tc_1O_D) + \nu(Tc_2O_D) + \nu(Tc_3O_D)]$		
		$\rho_w(O_BTc_1F_4) + \rho_r(O_BTc_2F_4) + \rho_r(O_BTc_3F_4)$	$\nu_8(A_1)$	193(3)[<1]
196(4)[<0.01]	$\nu_{20}(E)$	$\rho_r(O_ATc_1O_B) + \rho_r(O_AO_BTc_2O_C) + \rho_r(O_AO_BTc_3O_C)$		
		$[\rho_r(O_CTc_1O_B) + \rho_r(O_ATc_2O_C) + \rho_r(O_AO_BTc_3O_C)] + [\nu(Tc_1F_2) + \nu(Tc_2F_2) - \nu(Tc_2F_3) + \nu(Tc_3F_3)]$	$\nu_{20}(E)$	188(2)[<0.1]
166(1)[1]	$\nu_9(A_1)$	$[\nu(Tc_1F_2) + \nu(Tc_2F_2)] + [\nu(Tc_2F_3) + \nu(Tc_3F_3)] + [\nu(Tc_3F_1) + \nu(Tc_1F_1)] + [\nu(Tc_1O_D) + \nu(Tc_2O_D) + \nu(Tc_3O_D)] + \rho_r(O_AO_BTc_1O_C) + \rho_r(O_AO_BTc_2O_C) + \rho_r(O_AO_BTc_3O_C)$		
		$\rho_r(O_AO_BTc_1O_C) + \rho_r(O_AO_BTc_2O_C) + \rho_r(O_AO_BTc_3O_C)$	$\nu_9(A_1)$	132(1)[<1]
130(<0.1)[<0.1]	$\nu_{21}(E)$	$\rho_r(O_AO_BTc_1O_C) - \rho_r(O_AO_BTc_2O_C)$	$\nu_{21}(E)$	108(<1)[<0.1]
92(<1)[<1]	$\nu_{22}(E)$	deformation modes	$\nu_{22}(E)$	97(1)[<0.1]
83(1)[1]	$\nu_{23}(E)$		$\nu_{23}(E)$	57(<1)[<1]

[a]Frequencies are in cm^{-1}. [b]Values in parentheses denote calculated Raman intensities ($Å^4\ u^{-1}$). Values in square brackets denote calculated infrared intensities (km mol^{-1}). The B3LYP/aug-cc-pVTZ(–PP) method was used. [c]The abbreviations denote stretch (ν), bend (δ), rock (ρ_r), and wag (ρ_w).

Table S5. Experimental Geometrical Parameters for the $[\{TcO_3(\mu\text{-}F)\}_3(\mu_3\text{-}F)]^-$ Anion in $K[\{TcO_3(\mu\text{-}F)\}_3(\mu_3\text{-}F)]\cdot 1.5TcO_3F$ and Calculated Geometrical Parameters for the $[\{TcO_3(\mu\text{-}F)\}_3(\mu_3\text{-}O)]^{2-}$ and $[\{TcO_3(\mu\text{-}F)\}_3(\mu_3\text{-}F)]^-$ Anions

calcd[a,b]				exptl[c]	
$[\{TcO_3(\mu\text{-}F)\}_3(\mu_3\text{-}O)]^{2-}$		$[\{TcO_3(\mu\text{-}F)\}_3(\mu_3\text{-}F)]^-$			
Bond Lengths (Å)					
$Tc_1–O_A$	1.693	$Tc_1–O_A$	1.680	$Tc_1–O_{11}$	1.685(4)
$Tc_1–O_B$	1.700	$Tc_1–O_B$	1.681	$Tc_1–O_{12}$	1.677(4)
$Tc_1–O_C$	1.693	$Tc_1–O_C$	1.680	$Tc_1–O_{13}$	1.682(4)
$Tc_2–O_A$	1.693	$Tc_2–O_A$	1.680	$Tc_2–O_{21}$	1.680(4)
$Tc_2–O_B$	1.700	$Tc_2–O_B$	1.681	$Tc_2–O_{22}$	1.683(4)
$Tc_2–O_C$	1.693	$Tc_2–O_C$	1.680	$Tc_2–O_{23}$	1.687(4)
$Tc_3–O_A$	1.693	$Tc_3–O_A$	1.680	$Tc_3–O_{33}$	1.667(4)
$Tc_3–O_B$	1.700	$Tc_3–O_B$	1.681	$Tc_3–O_{32}$	1.685(4)
$Tc_3–O_C$	1.693	$Tc_3–O_C$	1.680	$Tc_3–O_{31}$	1.691(4)
$Tc_1–O_D$	2.096	$Tc_1–F_4$	2.302	$Tc_1–F_{10}$	2.266(3)
$Tc_2–O_D$	2.096	$Tc_2–F_4$	2.302	$Tc_2–F_{10}$	2.246(3)
$Tc_3–O_D$	2.096	$Tc_3–F_4$	2.302	$Tc_3–F_{10}$	2.223(3)
$Tc_1–F_1$	2.165	$Tc_1–F_1$	2.128	$Tc_1–F_1$	2.132(3)
$Tc_1–F_2$	2.165	$Tc_1–F_2$	2.128	$Tc_1–F_2$	2.102(3)
$Tc_2–F_2$	2.165	$Tc_2–F_2$	2.128	$Tc_2–F_2$	2.098(3)
$Tc_2–F_3$	2.165	$Tc_2–F_3$	2.128	$Tc_2–F_3$	2.113(3)
$Tc_3–F_3$	2.165	$Tc_3–F_3$	2.128	$Tc_3–F_3$	2.110(3)
$Tc_3–F_1$	2.165	$Tc_3–F_1$	2.128	$Tc_3–F_1$	2.112(3)
Bond Angles (deg)					
$O_A–Tc_1–O_B$	104.9	$O_A–Tc_1–O_B$	105.8	$O_{12}–Tc_1–O_{13}$	105.5(2)
$O_B–Tc_1–O_C$	104.9	$O_B–Tc_1–O_C$	105.8	$O_{12}–Tc_1–O_{11}$	105.4(2)
$O_C–Tc_1–O_A$	102.8	$O_C–Tc_1–O_A$	103.6	$O_{13}–Tc_1–O_{11}$	104.1(2)
$O_A–Tc_1–O_D$	95.1	$O_A–Tc_1–F_4$	89.1	$O_{11}–Tc_1–F_{10}$	88.1(2)
$O_B–Tc_1–O_D$	147.5	$O_B–Tc_1–F_4$	155.3	$O_{12}–Tc_1–F_{10}$	157.3(2)
$O_C–Tc_1–O_D$	95.1	$O_C–Tc_1–F_4$	89.1	$O_{13}–Tc_1–F_{10}$	88.2(2)
$O_A–Tc_2–O_B$	104.9	$O_A–Tc_2–O_B$	105.8	$O_{21}–Tc_2–O_{22}$	105.5(2)
$O_B–Tc_2–O_C$	104.9	$O_B–Tc_2–O_C$	105.8	$O_{22}–Tc_2–O_{23}$	105.9(2)
$O_C–Tc_2–O_A$	102.8	$O_C–Tc_2–O_A$	103.6	$O_{23}–Tc_2–O_{21}$	103.6(2)
$O_A–Tc_2–O_D$	95.1	$O_A–Tc_2–F_4$	89.1	$O_{23}–Tc_2–F_{10}$	86.9(2)
$O_B–Tc_2–O_D$	147.5	$O_B–Tc_2–F_4$	155.3	$O_{21}–Tc_2–F_{10}$	157.3(2)
$O_C–Tc_2–O_D$	95.1	$O_C–Tc_2–F_4$	89.1	$O_{22}–Tc_2–F_{10}$	89.0(2)
$O_A–Tc_3–O_B$	104.9	$O_A–Tc_3–O_B$	105.8	$O_{33}–Tc_3–O_{31}$	104.9(2)
$O_B–Tc_3–O_C$	104.9	$O_B–Tc_3–O_C$	105.8	$O_{32}–Tc_3–O_{33}$	105.3(2)
$O_C–Tc_3–O_A$	102.8	$O_C–Tc_3–O_A$	103.6	$O_{31}–Tc_3–O_{32}$	103.5(2)
$O_A–Tc_3–O_D$	89.1	$O_A–Tc_3–F_4$	89.1	$O_{31}–Tc_3–F_{10}$	88.0(2)
$O_B–Tc_3–O_D$	147.5	$O_B–Tc_3–F_4$	155.3	$O_{33}–Tc_3–F_{10}$	157.3(2)
$O_C–Tc_3–O_D$	95.1	$O_C–Tc_3–F_4$	89.1	$O_{32}–Tc_3–F_{10}$	89.2(2)
$O_A–Tc_1–F_2$	87.7	$O_A–Tc_1–F_2$	87.3	$O_{12}–Tc_1–F_2$	93.0(2)
$O_B–Tc_1–F_2$	85.2	$O_B–Tc_1–F_2$	92.7	$O_{11}–Tc_1–F_2$	87.9(2)
$O_C–Tc_1–F_2$	162.7	$O_C–Tc_1–F_2$	154.6	$O_{13}–Tc_1–F_2$	154.0(2)
$O_D–Tc_1–F_2$	70.0	$F_4–Tc_1–F_2$	67.9	$F_{10}–Tc_1–F_2$	68.9(1)
$O_A–Tc_1–F_1$	162.7	$O_A–Tc_1–F_1$	154.6	$O_{11}–Tc_1–F_1$	154.6(2)

Table S5. (continued…)

O_B–Tc_1–F_1	85.2	O_B–Tc_1–F_1	92.7	O_{12}–Tc_1–F_1	94.1(2)
O_C–Tc_1–F_1	87.7	O_C–Tc_1–F_1	87.3	O_{13}–Tc_1–F_1	85.8(2)
O_D–Tc_1–F_1	70.0	F_4–Tc_1–F_1	67.9	F_{10}–Tc_1–F_1	68.5(1)
O_A–Tc_2–F_2	87.5	O_A–Tc_2–F_2	87.3	O_{21}–Tc_2–F_2	93.5(2)
O_B–Tc_2–F_2	85.2	O_B–Tc_2–F_2	92.7	O_{22}–Tc_2–F_2	87.6(2)
O_C–Tc_2–F_2	162.7	O_C–Tc_2–F_2	154.6	O_{23}–Tc_2–F_2	153.7(2)
O_D–Tc_2–F_2	70.0	F_4–Tc_2–F_2	67.9	F_{10}–Tc_2–F_2	69.3(1)
O_A–Tc_2–F_3	162.7	O_A–Tc_2–F_3	154.6	O_{22}–Tc_2–F_3	155.1(2)
O_B–Tc_2–F_3	85.2	O_B–Tc_2–F_3	92.7	O_{21}–Tc_2–F_3	92.3(2)
O_C–Tc_2–F_3	87.7	O_C–Tc_2–F_3	87.3	O_{23}–Tc_2–F_3	87.6(2)
O_D–Tc_2–F_3	70.0	F_4–Tc_2–F_3	67.9	F_{10}–Tc_2–F_3	69.2(1)
O_A–Tc_3–F_3	162.7	O_A–Tc_3–F_3	154.6	O_{32}–Tc_3–F_3	156.5(2)
O_B–Tc_3–F_3	85.2	O_B–Tc_3–F_3	92.7	O_{31}–Tc_3–F_3	92.1(2)
O_C–Tc_3–F_3	87.7	O_C–Tc_3–F_3	87.3	O_{33}–Tc_3–F_3	86.7(2)
O_D–Tc_3–F_3	70.0	F_4–Tc_3–F_3	67.9	F_{10}–Tc_3–F_3	69.7(1)
O_A–Tc_3–F_1	87.7	O_A–Tc_3–F_1	87.3	O_{32}–Tc_3–F_1	87.5(2)
O_B–Tc_3–F_1	85.2	O_B–Tc_3–F_1	92.7	O_{33}–Tc_3–F_1	93.2(2)
O_C–Tc_3–F_1	162.7	O_C–Tc_3–F_1	154.6	O_{31}–Tc_3–F_1	155.2(2)
O_D–Tc_3–F_1	68.0	F_4–Tc_3–F_1	67.9	F_{10}–Tc_3–F_1	69.7(1)
F_1–Tc_1–F_2	79.1	F_1–Tc_1–F_2	74.5	F_1–Tc_1–F_2	74.6(1)
F_2–Tc_2–F_3	79.1	F_2–Tc_2–F_3	74.5	F_2–Tc_2–F_3	73.9(1)
F_3–Tc_3–F_1	79.1	F_3–Tc_3–F_1	74.5	F_3–Tc_3–F_1	75.6(1)
Tc_1–O_D–Tc_2	110.0	Tc_1–F_4–Tc_2	103.5	Tc_1–F_{10}–Tc_2	103.0(1)
Tc_2–O_D–Tc_3	110.0	Tc_2–F_4–Tc_3	103.5	Tc_2–F_{10}–Tc_3	104.2(1)
Tc_3–O_D–Tc_1	110.0	Tc_3–F_4–Tc_1	103.5	Tc_3–F_{10}–Tc_1	105.0(1)
Tc_1–F_2–Tc_2	104.9	Tc_1–F_2–Tc_2	117.3	Tc_1–F_2–Tc_2	114.4(1)
Tc_2–F_3–Tc_3	104.9	Tc_2–F_3–Tc_3	117.3	Tc_2–F_3–Tc_3	113.2(1)
Tc_3–F_1–Tc_1	104.9	Tc_3–F_1–Tc_1	117.3	Tc_3–F_1–Tc_1	114.1(1)

[a]For the atom labeling scheme, see Figure S5. [b]The B3LYP/aug-cc-pVTZ(–PP) method was used. [c]For the atom labeling scheme see Ref 13.

Complete References 49, 50 and 56

(49) Frisch, M. J.; Trucks, G. W.; Schlegel, H. B.; Scuseria, G. E.; Robb, M. A.;. Cheeseman, J. R;Zakrzewski, V. G.; Montgomery, J. A.; Stratmann, Jr., R. E.; Burant, J. C.; Dapprich, S.; Millam, J. M.; Daniels, A. D.; Kudin, K. N.; Strain, M. C.; Farkas, O.; Tomasi, J.; Barone, V.;Cossi, M.; Cammi, R.; Mennucci, B.; Pomelli, C.; Adamo, C.; Clifford, S.; Ochterski, J.; Petersson, G. A.; Ayala, P. Y.; Cui, Q.; Morokuma, K.; Salvador, P.; Dannenberg, J. J.;Malick, D. K.; Rabuck, A. D.; Raghavachari, K.; Foresman, J. B.; Cioslowski, J. V.; Ortiz, A.; Baboul, G.; Stefanov, B. B.; Liu, G.; Liashenko, A.; Piskorz, P. K. I.; Gomperts, R.;Martin, R. L.; Fox, D. J.; Keith, T.; Al-Laham, M. A.; Peng, C. Y.; Nanayakkara, A.; Challacombe, M.; Gill, P. M. W.; Johnson, B.; Chen, W.; Wong, M. W.; Andres, J. L; Gonzalez, C.; Head-Gordon, M.; Replogle, E. S.; Pople, J. A. *Gaussian 98*, Revision A.11; Gaussian, Inc.: Pittsburgh, PA, 2004 (**g03_D.01**).

(50) Frisch, M. J.; Trucks, G. W.; Schlegel, H. B.; Scuseria, G. E.; Robb, M. A.; Cheeseman, J. R.; Scalmani, G.; Barone, V.; Mennucci, B.; Petersson, G. A.; Nakatsuji, H.; Caricato, M.; Li, X.; Hratchian, H. P.; Izmaylov, A. F.; Bloino, J.; Zheng, G.; Sonnenberg, J. L.; Hada, M.; Ehara, M.; Toyota, K.; Fukuda, R.; Hasegawa, J.; Ishida, M.; Nakajima, T.; Honda, Y.; Kitao, O.; Nakai, H.; Vreven, T.; Montgomery, J. A.; Peralta, Jr., J. E.; Ogliaro, F.; Bearpark, M.; Heyd, J. J.; Brothers, E.; Kudin, K. N.; Staroverov, V. N.; Keith, T.; Kobayashi, R.; Normand, J.; Raghavachari, K.; Rendell, A.; Burant, J. C.; Iyengar, S. S.; Tomasi, J.; Cossi, M.; Rega, N.; Millam, J. M.; Klene, M.; Knox, J. E.; Cross, J. B.; Bakken, V.; Adamo, C.; Jaramillo, J.; Gomperts, R.; Stratmann, R. E.; Yazyev, O.; Austin, A. J.; Cammi, R.; Pomelli, C.; Ochterski, J. W.; Martin, R. L.; Morokuma, K.; Zakrzewski, V. G.; Voth, G. A.; Salvador, P.; Dannenberg, J. J.; Dapprich, S.; Daniels, A. D.; Farkas, O.; Foresman, J. B.; Ortiz, J. V.; Cioslowski, J.; Fox, D. J. Gaussian, Inc., Wallingford CT, 2010 (**g09_C.01**).

(56) Baerends, E.J.; Ziegler, T.; Autschbach, J.; Bashford, D.; Bérces, A.; Bickelhaupt, F. M.; Bo, C.; Boerrigter, P. M.; Cavallo, L.; Chong, D. P.; Deng, L.; Dickson, R. M.; Ellis, D. E.; van Faassen, M.; Fan, L.; Fischer, T. H.; Fonseca Guerra, C.; Ghysels, A.; Giammona, A.; van Gisbergen, S. J. A.; Götz, A. W.; Groeneveld, J. A.; Gritsenko, O. V.; Grüning, M.; Gusarov, S.; Harris, F. E.; van den Hoek, P.; Jacob, C. R.; Jacobsen, H.; Jensen, L.; Kaminski, J. W.; van Kessel, G.; Kootstra, F.; Kovalenko, A.; Krykunov, M. V.; van Lenthe, E.; McCormack, D. A.; Michalak, A.; Mitoraj, M.; Neugebauer, J.; Nicu, V. P.; Noodleman, L.; Osinga, V. P.; Patchkovskii, S.; Philipsen, P. H. T.; Post, D.; Pye, C. C.; Ravenek, W.; Rodríguez, J. I.; Ros, P.; Schipper, P. R. T.; Schreckenbach, G.; Seldenthuis, J. S.; Seth, M.; Snijders, J. G.; Solà, M.; Swart, M.; Swerhone, D.; te Velde, G.; Vernooijs, P.; Versluis, L.; Visscher, L.; Visser, O.; Wang, F.; Wesolowski, T. A.; van Wezenbeek, E. M.; Wiesenekker, G.; Wolff, S. K.; Woo, T. K.; Yakovlev, A. L. **ADF 2010**, SCM, Theoretical Chemistry, Vrije Universiteit, Amsterdam, The Netherlands, http://www.scm.com.